

Article

The Impact of Maternal SARS-CoV-2 Infection Next to Pre-Immunization with Gam-COVID-Vac (Sputnik V) Vaccine on the 1-Day-Neonate's Blood Plasma Small Non-Coding RNA Profile: A Pilot Study

Angelika V. Timofeeva ^{*}, Ivan S. Fedorov, Vitaliy V. Chagovets, Victor V. Zubkov, Mziya I. Makieva, Anna B. Sugak, Vladimir E. Frankevich and Gennadiy T. Sukhikh

FSBI, National Medical Research Center for Obstetrics, Gynecology and Perinatology Named after Academician V.I. Kulakov, Ministry of Healthcare of The Russian Federation, Ac. Oparina 4, Moscow 117997, Russia; is_fedorov@oparina4.ru (I.S.F.); v_chagovets@oparina4.ru (V.V.C.); v_zubkov@oparina4.ru (V.V.Z.); m_makieva@oparina4.ru (M.I.M.); a_sugak@oparina4.ru (A.B.S.); v_frankevich@oparina4.ru (V.E.F.); g_sukhikh@oparina4.ru (G.T.S.)

* Correspondence: v_timofeeva@oparina4.ru or avtimofeeva28@gmail.com; Tel.: +7-495-531-4444



Citation: Timofeeva, A.V.; Fedorov, I.S.; Chagovets, V.V.; Zubkov, V.V.; Makieva, M.I.; Sugak, A.B.; Frankevich, V.E.; Sukhikh, G.T. The Impact of Maternal SARS-CoV-2 Infection Next to Pre-Immunization with Gam-COVID-Vac (Sputnik V) Vaccine on the 1-Day-Neonate's Blood Plasma Small Non-Coding RNA Profile: A Pilot Study. *COVID* **2022**, *2*, 837–857. <https://doi.org/10.3390/covid2070061>

Academic Editor: Arnon Blum

Received: 2 June 2022

Accepted: 20 June 2022

Published: 24 June 2022

Publisher's Note: MDPI stays neutral with regard to jurisdictional claims in published maps and institutional affiliations.



Copyright: © 2022 by the authors. Licensee MDPI, Basel, Switzerland. This article is an open access article distributed under the terms and conditions of the Creative Commons Attribution (CC BY) license (<https://creativecommons.org/licenses/by/4.0/>).

Abstract: The antenatal and postnatal effects of maternal SARS-CoV-2 on the fetus outcomes, especially in the case of maternal pre-vaccination against this infection, are still under investigation. Such effects may be due to placental insufficiency caused by maternal hypoxia and inflammatory response associated with SARS-CoV-2, and/or be a direct cytopathic effect of the virus. In this work, we studied the profile of small non-coding RNAs (sncRNAs) in the blood plasma of a newborn from a mother who had SARS-CoV-2 at the 22nd week of gestation after immunization with Gam-COVID-Vac (Sputnik V). The fetus had ultrasound signs of hypertrophy of the right heart and hydropericardium 4 weeks after infection of the mother with SARS-CoV-2, as well as cysts of the cerebral vascular plexuses by the time of birth. Taking this into account, we compared the sncRNA profile of this newborn on the first postpartum day with that of neonates born to COVID-19-negative women with different perinatal outcomes: severe cardiovascular and/or neurological disorders, or absence of any perinatal complications. According to next-generation sequencing data, we found that the fetus born to a COVID-19-affected mother pre-immunized with Gam-COVID-Vac (Sputnik V) vaccine differs from newborns with severe cardiovascular and/or nervous system abnormalities either in multidirectional changes in circulating sncRNAs or in less pronounced unidirectional changes in the level of sncRNAs relative to control samples. Considering this, it can be concluded that maternal vaccination against SARS-CoV-2 before pregnancy has a protective effect in preventing antenatal development of pathological processes in the cardiovascular and nervous systems of the neonate associated with COVID-19.

Keywords: SARS-CoV-2; COVID-19; neonate; small non-coding RNA; next generation sequencing; cardiovascular system; nervous system; blood plasma

1. Introduction

According to the World Health Organization (WHO), COVID-19 caused by SARS-CoV-2, was declared a global pandemic on 11 March 2020, with more than 281 million cases in 223 countries and more than 5.4 million deaths reported globally [1]. Despite global mass vaccination efforts to prevent COVID-19, the emergence of new SARS-CoV-2 variants—Alpha (B.1.1.7), Beta (B.1.351), Gamma (P.1), Delta (B.1.617.2), and Omicron (B.1.1.529) poses a serious threat to public health according to the recent epidemiological data presented by the WHO on 11 December 2021. Issues of managing pregnancy in the pandemic remain open, namely: vaccination regimens, treatment in case of infection, and antenatal and

postnatal complications in the fetus. Recent studies have shown that vertical transmission of SARS-CoV-2 occurs in approximately 2–8% of cases [2–5]. This low percentage can be explained by the fact that the placenta is a strong physical and immunological barrier against SARS-CoV-2 infection during pregnancy [5–7]. The barrier function is provided by four factors. (i) The presence of a multinucleated syncytiotrophoblast (STB), which is periodically renewed by fusion of proliferating villous cytotrophoblasts (vCTB) leading to the disappearance of intercellular gap junctions. STB is covered by a dense network of branched microvilli [8] and does not express caveolin-1 [9], thus preventing virus penetration and local inflammation. (ii) The presence of a basement membrane underlying the vCTB layer [8]. (iii) Low incidence of colocalization of membrane-associated angiotensin-converting enzyme (ACE2) and transmembrane serine protease 2 (TMPRSS2) in STB, vCTB, decidual perivascular and stromal cells [10], which accounts for the low probability of transplacental infection. (iv) Transplacental transmission of maternal humoral immunity to the fetus due to the expression of FcRn and FcR3 receptors for IgG on the STB surface, starting from 16 weeks of pregnancy [11,12].

However, the possibility of the viral transmission through the maternal–fetal interface of placenta may still occur in the first and third trimesters of pregnancy due to incomplete or reduced STB formation, respectively [13,14]. Moreover, it was suggested that viral entry into placental cells may occur through a combination of ACE2 and a noncanonical cell-entry mediator [15]. In addition, destruction of STB and a decrease in the protective properties of the placenta can be caused by exposure to a high maternal load of SARS-CoV-2, which can trigger a “cytokine storm” with a surge of pro-inflammatory cytokines, including IFN- γ , TNF- α , IL-2, -6, -7, -10 [16]. These processes damage placental tissue, and/or may cause maternal hypoxia, leading to the placenta hypoperfusion/ischemia and the development of clinical and laboratory symptoms similar to preeclampsia [17], miscarriage, intrauterine death, fetal growth restriction, fetal inflammatory response, respiratory failure, and such long-term complication as neurosensorial developmental delay [6,18–27]. Meta-analysis of the 1008 pregnancies [28] and case–control study of 81 pregnant mothers [29] revealed placental histopathologic anomalies such as maternal and fetal vascular malperfusion, increased perivillous fibrin, intervillous thrombosis, and villous edema owing to SARS-CoV-2 maternal infection. Profiling of mRNA expression in placental tissues with a high SARS-CoV-2 titer compared to SARS-CoV-2-positive placentas without severe injury revealed high expression of genes involved in innate and adaptive antiviral immunity as well as chemotactic and inflammatory response, suggesting that they reflect different neonatal outcomes and differentiate perinatal asphyxia from asymptomatic neonates [30]. It is possible that in COVID-positive woman pregnant with a bi-chorial, bi-amniotic twin, it was the differences in the mRNA expression profile of the two placentas despite their identical histological and immunohistochemical characteristics that caused a different neonatal outcome in fetuses: the birth of the first living and viable fetus and the birth of the second fetus with severe intra-partum distress and death [31]. The maternal-fetal interaction at the molecular level in the case of a SARS-CoV-2 positive mother has not yet been studied. The only relevant investigation published recently revealed distinct lipidomic and metabolomic profiles in the blood plasma of neonates born to SARS-CoV-2 positive mothers at birth but without evidence of viral infection compared to those of neonates born to uninfected mothers using GC-MS and UHPLC-TOF/MS [32].

To the best of our knowledge, no studies have been conducted on the profile of small non-coding RNA (sncRNA) in neonates born to pregnant women who test positive for SARS-CoV-2. These regulatory non-coding RNAs, in particular miRNA and piRNA, have been suggested as promising biomarkers and therapeutic targets, mainly due to their condition- and cell-specific expression, as well as their impact on the network of signaling pathways at epigenetic, transcriptional, and posttranscriptional levels [33–37]. The effect of SARS-CoV-2 on the host miRNA profile was only investigated in blood plasma and placenta of pregnant women infected with SARS-CoV-2 [38] or in blood plasma/serum of COVID-19 patients [39,40].

Since differences in the molecular profiles of the blood of neonates born to COVID-19-infected women during pregnancy without preliminary vaccination against SARS-CoV-2 have already been demonstrated [32], the present study was aimed to analyze the miRNA and piRNA expression profiles in the blood plasma of the first-day neonate born to a COVID-19-affected woman pre-immunized with Gam-COVID-Vac vaccine in comparison with newborns from COVID-19-negative women with different perinatal outcomes. The results of this work are important in understanding the need for vaccination with currently available COVID-19 vaccines before and/or in pregnancy to avoid severe maternal and neonatal complications associated with SARS-CoV-2 infection such as premature delivery, pre-eclampsia, stillbirth, and neonatal and maternal mortality [41]. Moreover, up to date, the degree to which titers of maternal immunoglobulin G antibody, passed to the fetus through placenta, correlate with infant protection from SARS-CoV2 infection is still unknown [42].

2. Materials and Methods

2.1. Patients

In total, 13 SARS-CoV-2-negative neonates born to women unaffected by SARS-CoV-2 infection during pregnancy and 1 SARS-CoV-2-negative neonate born to mother who was pre-immunized with Gam-COVID-Vac (Sputnik V) vaccine before pregnancy and had COVID-19 in the second trimester were enrolled in the study (briefly in Table 1, in more detail in Table S1). Among SARS-CoV-2-unaffected mothers, 11 were characterized by premature delivery at 35–36.4 week of gestation (GW) by Caesarean section (10 cases) or spontaneously (1 case) in conjunction with pathological invasion of placenta (7 cases), low placentation and preeclampsia (1 case), premature rupture of the fetal membrane (1 case), placenta previa and small uterine myoma (1 case), chronic arterial hypertension and primary antiphospholipid syndrome (1 case), and the other two SARS-CoV-2-unaffected mothers were characterized by timely spontaneous or operative delivery at 40.1 GW and 38.4 GW, respectively. Newborns from SARS-CoV-2-unaffected mothers were either apparently healthy (3 cases), or had central nervous system (CNS) and/or cardiovascular disorders (10 cases), among which were the following: intraventricular hemorrhage in the antenatal or early neonatal period, subependymal cysts, vascular plexus cysts, syndrome of CNS function depression with delayed formation of unconditioned reflex activity, myocardial hypertrophy, hydropericardium, arterial hypotension, pulmonary hypertension, and posthypoxic sinus node dysfunction. A term infant born to a mother who had been vaccinated against SARS-CoV-2 prior to pregnancy and had COVID-19 at 22–23 GW showed moderate right ventricular hypertrophy and hydropericardium at 26–27 GW, and two cerebral plexus cysts were detected at birth.

The criteria for mild COVID-19 were the detection of SARS-CoV-2 RNA by polymerase chain reaction with reverse transcription (RT-PCR) in an oropharyngeal swab in combination with the following clinical manifestations: the temperature is not higher than subfebrile ($<38^{\circ}\text{C}$) and the absence of criteria for severe and moderate infection. The criteria for moderate disease were the detection of SARS-CoV-2 RNA by RT-PCR in an oropharyngeal swab in combination with any of the following clinical manifestations: the temperature is above subfebrile ($>38^{\circ}\text{C}$); respiratory rate > 22 per minute; dyspnea exertional, oxygen saturation (SpO₂) $< 95\%$; presence of pneumonia on computed tomography (CT) with minimal to moderate lung lesion volume (CT 1–2). Criteria of the disease severity were the detection of SARS-CoV-2 RNA by RT-PCR in oropharyngeal swab in combination with any of the following clinical manifestations: respiratory rate $> 30/\text{min}$; SpO₂ $\leq 93\%$; PaO₂/FiO₂ ≤ 300 mm Hg; decreased level of consciousness; agitation; unstable hemodynamics (systolic blood pressure < 90 mm Hg or diastolic blood pressure < 60 mm Hg, diuresis less than 20 mL/h); changes in the lungs on CT (X-ray), typical for viral lesions (lesion volume is significant or subtotal; CT 3–4); quick Sequential Organ Failure Assessment (qSOFA) > 2 points (Temporary Methodological Recommendations “Prevention, Diagnosis and Treatment of New Coronavirus Infection (COVID-19)” of the Ministry of Health of the Russian Federation. Version 12 (21 September 2021), https://static-0.minzdrav.gov.ru/system/attachments/attaches/000/058/075/original/BMP_COVID-19_V12.pdf (accessed on 26 October 2021).

Table 1. Clinical characteristics of newborns and their mothers.

1st Day Newborn Blood Plasma Sample ID	Maternal Age	Mode of Delivery	Maternal Diagnosis	GW ¹	Newborn			APGAR Score at the 1st and 5th Minutes	CNS Disorder	Cardiovascular Disorder
					Gender	Weight	Growth			
#3	22	Caesarean section	placenta previa, placenta increta	35	female	2300	48	7 and 7	Yes	Yes
#20	32	Caesarean section	Gestational arterial hypertension. Placenta previa. Placenta accreta. Low placentation.	35.1	female	2850	47	7 and 8	Yes	No
#41	28	Caesarean section	Preeclampsia. Chronic arterial hypertension.	35.1	male	3144	51	8 and 9	Yes	Yes
#151	36	Caesarean section	Complete placenta previa. Placenta percreta.	35.4	female	3062	50	8 and 9	Yes	No
#52	27	Caesarean section	Central placenta previa. Placenta accreta.	36.4	male	2960	48	8 and 8	Yes	Yes
#129	37	Caesarean section	Placenta previa and placenta accreta	36	male	2758	49	8 and 9	Yes	Yes
#29	21	Caesarean section	Placenta previa. Small uterine myoma.	36	male	2780	52	8 and 8	Yes	Yes
#26	36	Caesarean section	Placenta previa. Placenta percreta.	35	female	2480	49	7 and 7	No	Yes
#152	30	Caesarean section	Placenta previa. Placenta percreta	36.1	female	2670	52	8 and 9	Yes	Yes
#32	28	spontaneous delivery	premature rupture of the foetal membrane Chronic arterial	36	male	2625	47	7 and 8	Yes	Yes
#42	39	Caesarean section	hypertension. Primary antiphospholipid syndrome.	35.3	male	2480	49	8 and 8	No	No
#200	39	physiological delivery	Timely spontaneous delivery	40.1	male	3468	52	8 and 9	No	No
#201	26	Caesarean section	Chronic arterial hypertension.	38.4	male	3344	53	8 and 9	No	No
#202	38	physiological delivery	Condition after COVID-19 infection.	39.2	male	3402	52	8 and 9	Yes	Yes (only at 26–27 GW)

¹ GW—gestational week.

Virus identification was performed using SARS-CoV-2/SARS-CoV RT-PCR Kit (DNA-Technology, Russia, <https://www.dna-technology.ru/> (accessed on 4 May 2021).

The content of IgG antibodies in peripheral blood serum was determined by solid-phase enzyme immunoassay using a kit for detecting class G antibodies to SARS-CoV-2 spike protein (DS-IFA-ANTI-SARS-CoV-2-G (S), Diagnostic Systems Research and Production Association, Russia). The results were recorded on the Tecan Infinite F50 Absorbance Microplate Reader. The result was considered positive if the value was greater than 1.2.

All blood plasma samples were collected in FSBI “National Medical Research Center for Obstetrics, Gynecology, and Perinatology, named after Academician V.I. Kulakov” in 2021.

2.2. RNA Isolation from Peripheral Blood Plasma

Venous blood samples from pregnant women were collected into S-MONOVETTE® 2.7 mL, K3E EDTA tubes (SARSTEDT AG & Co., Nümbrecht, Germany, cat. No 05.1167.001), centrifuged for 20 min at 300 g (4 °C) followed by plasma collection and re-centrifugation for 10 min at 14,500 g. RNA was extracted from 200 µL of blood plasma using an miRNeasy Serum/Plasma Kit (Qiagen, Hilden, Germany, cat. No 217184).

2.3. cDNA Library Preparation and RNA Deep Sequencing

cDNA libraries were synthesized using 7 µL of the 14 µL total RNA column eluate (miRNeasy Serum/Plasma Kit, Qiagen, Hilden, Germany) and the NEBNext® Multiplex Small RNA Library Prep Set for Illumina® (Set1 and Set2, New England Biolab®, Frankfurt am Main, Germany), amplified for 19 PCR cycles, fractionated in polyacrylamide gel, and sequenced on the NextSeq 500 platform (Illumina, San Diego, CA, USA). The adapters were removed using Cutadapt software tool [43]. All trimmed reads shorter than 16 bp and longer than 50 bp were filtered out. The remaining reads were mapped to the GRCh38.p15 human genomes, miRBase v21 [44], and piRNABase (<https://www.pirnadb.org/> (accessed on 15 December 2021) with bowtie aligner [45]. Aligned reads were counted using the featureCount tool from the Subread package [46] and with the fracOverlap 0.9 option, so the whole read was forced to have 90% intersection with sncRNA features. Differential expression analysis of the sncRNA count data was performed with the DESeq2 package [47].

2.4. Statistical Analysis of the Obtained Data

For statistical processing, we used scripts written in R language [46] in RStudio [48].

The Partial Least Squares Discriminant Analysis (PLS-DA) model [49] was developed to study differences in the level of miRNAs and piRNAs expression in peripheral blood plasma of neonates of the first day of life with different outcomes.

3. Results

3.1. The Results of Clinical and Instrumental Methods of Examination of a Neonate Born to COVID-19-Affected Mother Pre-Immunized with Gam-COVID-Vac (Sputnik V) Vaccine

A male neonate was born to a 38-year-old woman with COVID-19 who was pre-immunized with Gam-COVID-Vac (Sputnik V) prior to pregnancy. The first trimester of pregnancy was uneventful, but at the 22–23 GW the pregnant woman suffered a mild form of COVID-19 and received treatment with Fraxiparine, Vitamin D3, Vitamin C, Grippferon, and Chophytol due to an increase in liver transaminases. The third trimester proceeded without clinical features. The neonate was born by vaginal delivery at 39.2 GW with an Apgar score of 8 and 9 at the first and fifth minutes, respectively. Birth weight was 3402 g. The newborn’s condition was satisfactory. Tests for SARS-CoV-2 RNA by RT-PCR in placental tissue, neonatal, and maternal oropharyngeal swab were negative. The level of neonatal SARS-CoV-2 IgG was 12.1.

3.1.1. Laboratory Test Data of 1st Day Newborn

The results of biochemical analysis of the peripheral blood of a newborn on the first day after delivery, obtained using the BA400 BioSystems, are presented in Table 2. The increased

values of the following biochemical parameters are noteworthy: direct and total bilirubin, alanine aminotransferase (ALT), aspartate aminotransferase (AST), and lactate dehydrogenase (LDG).

Table 2. Results of biochemical analysis of the peripheral blood of a newborn on the first day.

Biochemical Indicator	Value	Reference Values
glucose, mmol/L	4.0	3.9–6.4
creatinin, $\mu\text{mol/L}$	26.7	35–62
direct bilirubin, $\mu\text{mol/L}$	6.6	0–5.5
alanine aminotransferase (ALT), U/L	103.3	0–40
aspartate aminotransferase (AST), U/L	71.4	0–40
alkaline phosphatase (ALP), U/L	203.1	50–360
gamma-glutamyl transferase (GGT), U/L	121.7	0–250
total bilirubin, $\mu\text{mol/L}$	293.8	3.4–21
lactate dehydrogenase (LDG), U/L	1513.3	300–730
uric acid, $\mu\text{mol/L}$	217.3	202–416

The results of a clinical analysis of peripheral blood when using Sysmex XN-350 are presented in Table 3. All values of clinical parameters were normal, except for a minor anisocytosis, indicating mild anemia in the newborn.

Table 3. Results of clinical analysis of peripheral blood of a newborn on the first day.

Indicator	Value	Reference Values
leukocytes/WBC, $\times 10^9/\text{L}$	10.51	5.9–17.5
erythrocytes/RBC, $\times 10^{12}/\text{L}$	5.00	3.9–5.9
hemoglobin/HGB, g/L	183	134–198
hematocrit/HCT, L/L	0.497	0.41–0.65
mean corpuscular volume/MCV, fL	99.4	88–140
mean corpuscular haemoglobin/MCH, pg	36.6	30–37
mean corpuscular hemoglobin concentration/MCHC, g/dL	36.8	28–36
erythrocyte anisocytosis SD/RDW-SD, fL	65.1	35.1–46.3
erythrocyte anisocytosis CV/RDW-CV	17.4	11.5–14.5
platelets/PLT, $\times 10^9/\text{L}$	286	218–419
platelet anisocytosis/PDW, fL	10.7	5–30
mean thrombocyte volume/MPV, fL	9.6	9.4–12.3
Platelet-Large Cell Ratio/P-LCR, %	22.5	13–43
thrombocrit/PCT, %	0.27	0.1–0.4
immature granulocytes (relative count)/IG%	1.2	0–1.9
neutrophilic leukocyte (relative count)/NEUT%	41.0	20.2–66.1
lymphocytes (relative count)/LYMPH%	39.5	24.9–67.6
monocytes (relative count)/MONO%	11.8	6.7–19.9
eosinophils (relative count)/EO%	6.0	0.3–5.2
basophils (relative count)/BASO%	0.5	0–1
immature granulocytes (absolute count)/IG, $\times 10^9/\text{L}$	0.13	0–0.28
neutrophilic leukocyte (absolute count)/NEUT, $\times 10^9/\text{L}$	4.31	1.73–7.75
lymphocytes (absolute count)/LYMPH, $\times 10^9/\text{L}$	4.15	1.75–7.53
monocytes (absolute count)/MONO, $\times 10^9/\text{L}$	1.24	0.52–1.77
eosinophils (absolute count)/EO, $\times 10^9/\text{L}$	0.63	0.12–0.66
basophils (absolute count)/BASO, $\times 10^9/\text{L}$	0.05	0–0.15

On the first day of the newborn's life, blood was taken from the peripheral vein and immunogram parameters were evaluated with the determination of the total number of lymphocytes, the major subpopulations of immunocompetent T cells (CD3+, CD3+CD4+, CD3+CD8+), B cells (CD19+), B1 cells (CD19+CD5+), NK cells (CD56+CD16+), and activated lymphocytes (CD3+HLA-DR+, CD3+CD25+). Phenotyping of peripheral blood lymphocytes was performed on a Gallios flow cytometer (Beckman Coulter, Brea, CA, USA) using monoclonal antibodies FITC- or PE-labeled monoclonal antibodies against CD3 (FITC), CD4 (PE), CD5 (PE), CD8 (PE), CD16 (PE), CD19 (FITC), CD56 (PE), CD25 (FITC), HLA-DR (FITC) antigen (Becton Dickinson and eBioscience, USA) using Kaluza software. The immunogram data are presented in Table 4.

Table 4. Quantification of the composition of the lymphocyte subpopulation.

Indicator	Value	Reference Values
leukocytes $\times 10^9/L$	10.51	5.9–17.5
lymphocytes (relative count) %	39.5	24.9–67.6
lymphocytes (absolute count) $\times 10^9/L$	4.15	1.75–7.53
CD3+ (T lymphocytes) (relative count) %	90.3	58–70
CD3+ (T lymphocytes) (absolute count) $\times 10^9/L$	3.75	1–5.3
CD3+CD4+ (T helper cells) (relative count) %	71.3	38–50
CD3+CD4+ (T helper cells) (absolute count) $\times 10^9/L$	2.96	0.7–3.8
CD3+CD8+ (cytotoxic T lymphocyte) (relative count) %	20.5	15–25
CD3+CD8+ (cytotoxic T lymphocyte) (absolute count) $\times 10^9/L$	0.85	0.3–1.9
CD3+CD4+/CD3+CD8+	3.5	1.5–2.9
CD19+ (B lymphocytes) (relative count) %	6.6	12–30
CD19+ (B lymphocytes) (absolute count) $\times 10^9/L$	0.27	0.2–2.3
CD3-CD16+CD56+ (NK cells) (relative count) %	1.1	5–15
CD3-CD16+CD56+ (NK cells) (absolute count) $\times 10^9/L$	0.05	0.09–1.12
CD3+CD16+CD56+ (relative count) %	0.1	0–10
CD3+CD16+CD56+ (absolute count) $\times 10^9/L$	0.00	0–0.8
CD19+CD5+ (relative count) %	1.5	3–8
CD19+CD5+ (absolute count) $\times 10^9/L$	0.06	0.05–0.6
CD56+ (relative count) %	0.9	5–15
CD56+ (absolute count) $\times 10^9/L$	0.04	0.09–1.12
CD3+HLA-Dr.+ (relative count) %	0.2	2–10
CD3+HLA-Dr.+ (absolute count) $\times 10^9/L$	0.01	0.02–0.4
CD3+CD25+ (relative count) %	5.9	0–7
CD3+CD25+ (absolute count) $\times 10^9/L$	0.24	0–0.14
CD3+CD56+ (relative count) %	0.1	0–10
CD3+CD56+ (absolute count) $\times 10^9/L$	0.00	0–0.4
CD25+ (relative count) %	6.2	1–10
CD25+ (absolute count) $\times 10^9/L$	0.26	0.01–0.4

The analysis of the immunogram parameters revealed the absence of lymphopenia, as in the case of severe COVID-19, while the balance between the immune cell populations of the newborn was affected by exposure to maternal SARS-CoV-2 secondary to vaccination against SARS-CoV-2: increased relative number of the T helper cells, increased ratio of T

helper cells and cytotoxic T lymphocyte, changes in the count and proportion of activated lymphocytes-increased absolute number of CD3+CD25+ T cells with receptors to IL-2 along with decreased absolute and relative number of CD3+HLA-Dr.+, decreased percentages of CD19+ B cells and CD19+CD5+ B-1 cells, decreased absolute and relative number of CD3⁻CD16+CD56+ natural killer cells.

3.1.2. Data of the Instrumental Methods of Examination

Fetal echocardiography revealed moderate hypertrophy of the right ventricle and hydropericardium in the fetus at 27 GW (Figure 1).

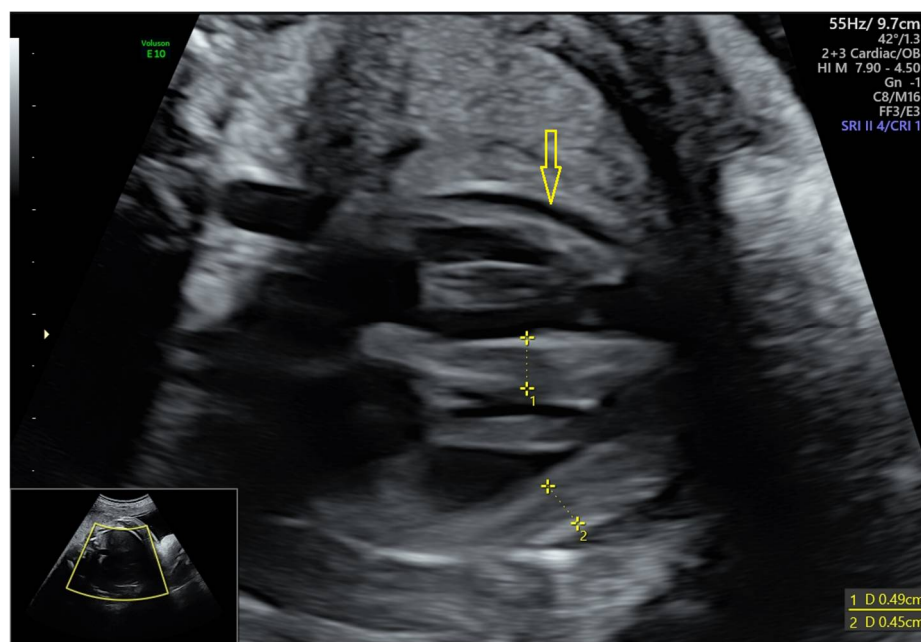


Figure 1. Ultrasound examination of the fetal heart at the 27 weeks of gestation. The dotted line indicates the thickness of the interventricular septum and the wall of the right ventricle. The arrow indicates fluid in the pericardial cavity up to 2 mm.

According to newborn's echocardiography at the first day after delivery, the left ventricle and left atrium were not enlarged; end-diastolic size of the left ventricle was 16 mm; end-systolic size of the left ventricle was 11 mm; ejection fraction of the left ventricle was 68%; the right heart was not expanded; mitral valve: thin and mobile leaflets, 11 mm fibrous ring, there was no regurgitation; trileaflet aortic valve was not changed, 1.5 mm Hg gradient, 7 mm fibrous ring, there was no regurgitation; aorta: the ascending section was not changed, the arch was not changed, the isthmus was 4.5 mm, the pressure gradient on the isthmus was 6 mm Hg; pulmonary valve: thin and mobile leaflets, 2.8 mm Hg gradient, 7.6 mm annulus fibrosus, minimal regurgitation; the pulmonary artery was not changed, the pressure gradient on the right pulmonary artery was 5 mm Hg, the pressure gradient on the left pulmonary artery was 5 mm Hg; tricuspid valve: thin and mobile leaflets, 12.5 mm annulus fibrosus, the degree of regurgitation was minimal; the interventricular septum was intact, the thickness of the interventricular septum was 4.7 mm; thickness of the posterior wall of the left ventricle was 2.6 mm, anterior wall of the right ventricle was 4.2 mm; interatrial septum: 2 mm open oval window, left-right reset; an additional chord of the left ventricle was revealed, no free fluid was found in the pericardial cavity.

According to the ultrasound examination of the newborn's abdominal organs, kidneys, and bladder, no organ pathology was detected at the first day after delivery.

According to newborn's neurosonography at the first day after delivery, the brain structures were located correctly; the structures were differentiated according to age; cavum

septi pellucida, the external liquor spaces, the interhemispheric fissure, the lateral ventricles, the III, and IV ventricles were not expanded; echogenicity was slightly increased over all sections of the periventricular region; C. magna—5 mm; subependymal sections and basal ganglia were not changed; two cysts, 4.8 mm and 2.4 mm, were detected in the choroid plexus on the left (Figure 2).

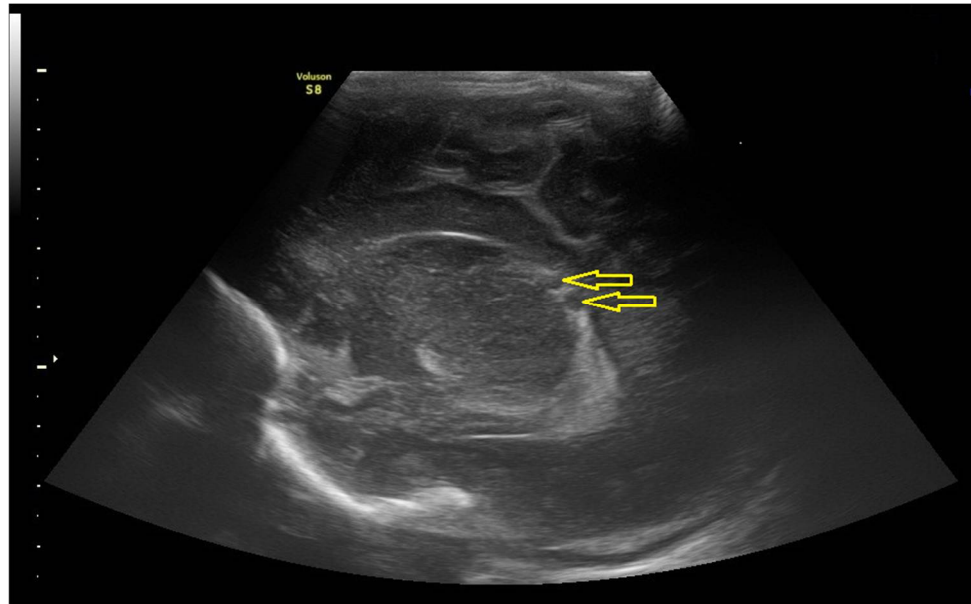


Figure 2. Neurosonography of the brain of a newborn on the first day after delivery. Arrows indicate choroid plexus cysts on the left.

Histological analysis of the placenta showed its correspondence to the gestational age; correct structure of the umbilical cord; predominance of angiogenesis with branching vessels in the chorion without any inflammatory changes; perivillous fibrin/fibrinoid deposits and decidual plate with increased deposition of fetal fibrinoid (Figure 3).

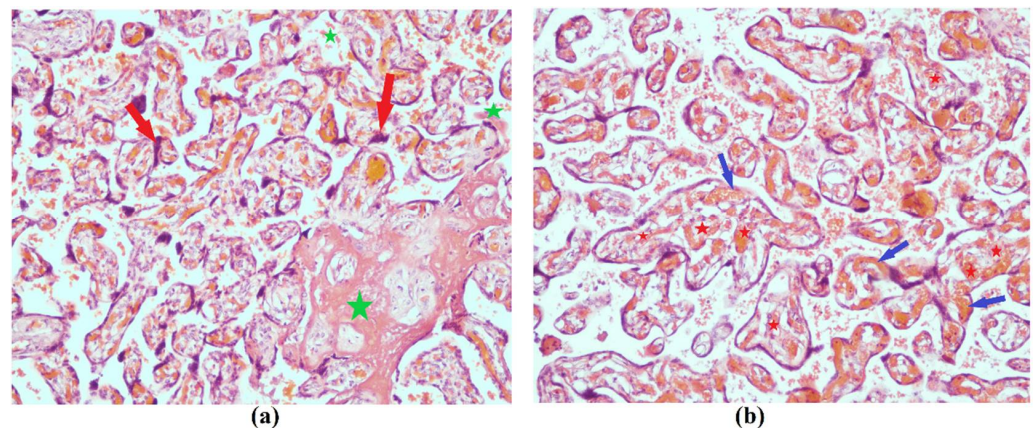


Figure 3. Microscopic characteristics of the H&E-stained sections of a 39.2 GW placenta; 100× magnification under microscopic examination. (a) Villi with syncytial knots (red arrows) and perivillous fibrin/fibrinoid deposits (green asterisks); (b) Villi with branching vessels and vascular congestion. Capillaries forming with villous syncytiotrophoblast vasculosyncytial membranes are indicated by blue arrows; capillaries lying separately from the syncytiotrophoblast are indicated by red asterisks.

3.2. Comparison of the Expression Profile of Small Non-Coding RNAs in Peripheral Blood of Neonates on the First Day of Life with Different Outcomes

In connection with the fact that a fetus born to a COVID-19-affected mother pre-immunized with Gam-COVID-Vac (Sputnik V) vaccine had a cardiovascular pathology (right ventricular hypertrophy and hydropericardium revealed 4 weeks after maternal SARS-CoV-2 infection at 22 GW followed by disappearance of echographic signs of cardiac pathology in the postpartum period) and brain pathology (two vascular plexus cysts according to neurosonographic data in the postpartum period), it seemed interesting to evaluate the expression profile of sncRNAs in the peripheral blood plasma of this 1-day-neonate with that of full-term healthy newborns and late preterm neonates (35–36.4 GW) with clinical manifestations of cardiovascular and/or central nervous system pathology. The research consisted of three main stages: (1) RNA isolation from 1-day-neonate blood plasma samples ($n = 13$); (2) quantitative analysis of sncRNA by deep sequencing to identify miRNA and piRNA expression changes in neonates with cardiovascular and/or central nervous system injury born to mothers with and without COVID-19 in comparison to healthy full-term neonates born to COVID-19-unaffected mothers; (3) functional analysis of target genes of sncRNAs associated with cardiovascular and central nervous system pathologies (Figure 4).

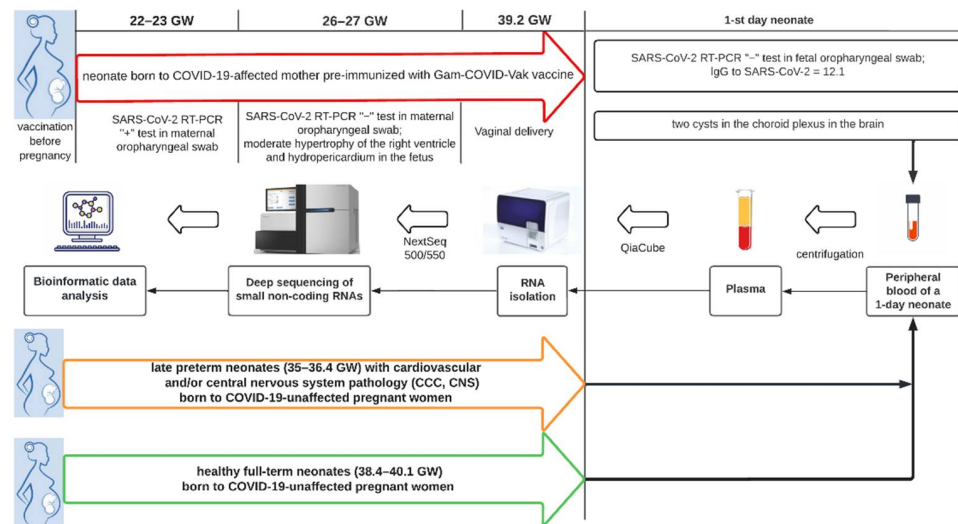


Figure 4. Flow diagram of the experimental design.

The PLS-DA model based on small RNA sequence data was developed to study differences in the expression level of miRNAs and piRNAs in peripheral blood plasma of neonates of the first day of life with different outcomes. Initially, the sncRNAs that contribute most (Variable Importance in Projection (VIP) score > 1 [50]) to the separation of a fetus born to a mother with COVID-19 and a full-term healthy newborns were selected (no data were provided). The resulting list of sncRNAs was then analyzed for the ability to differentiate between healthy neonates and neonates with diagnosed pathological changes in the cardiovascular and/or nervous systems in the postpartum period. A total of 19 miRNAs and 8 piRNAs were identified, which clearly distinguish the compared three types of samples in terms of their expression level in blood plasma: full-term neonate born to COVID-19-affected mother (sample #202), full-term healthy neonates born to SARS-CoV-2-negative mothers (samples #200 and #201), late preterm neonates with cardiovascular and/or central nervous system pathologies born to SARS-CoV-2-negative mothers (samples ## 3, 20, 26, 29, 41, 42, 52, 129, 151, and 152). The read counts of the sncRNAs presented in Table 5 were used to develop PLS-DA models depending on the direction of change in the expression level of sncRNAs in sample #202 and samples ## 3, 20, 26, 29, 41, 42, 52, 129, 151, and 152 relative to control samples #200 and #201, namely: decreased expression level

of sncRNAs in sample #202 and increased expression level in samples ## 3, 20, 26, 29, 41, 42, 52, 129, 151, and 152 (Figure 5A); increased expression level of sncRNAs in sample #202 and in samples ## 3, 20, 26, 29, 41, 42, 52, 129, 151, and 152 with more pronounced changes in the latter ones (Figure 5B); increased expression level of sncRNAs in sample #202 and in samples ## 3, 20, 26, 29, 41, 42, 52, 129, 151, and 152 with more pronounced changes in the former ones (Figure 5C).

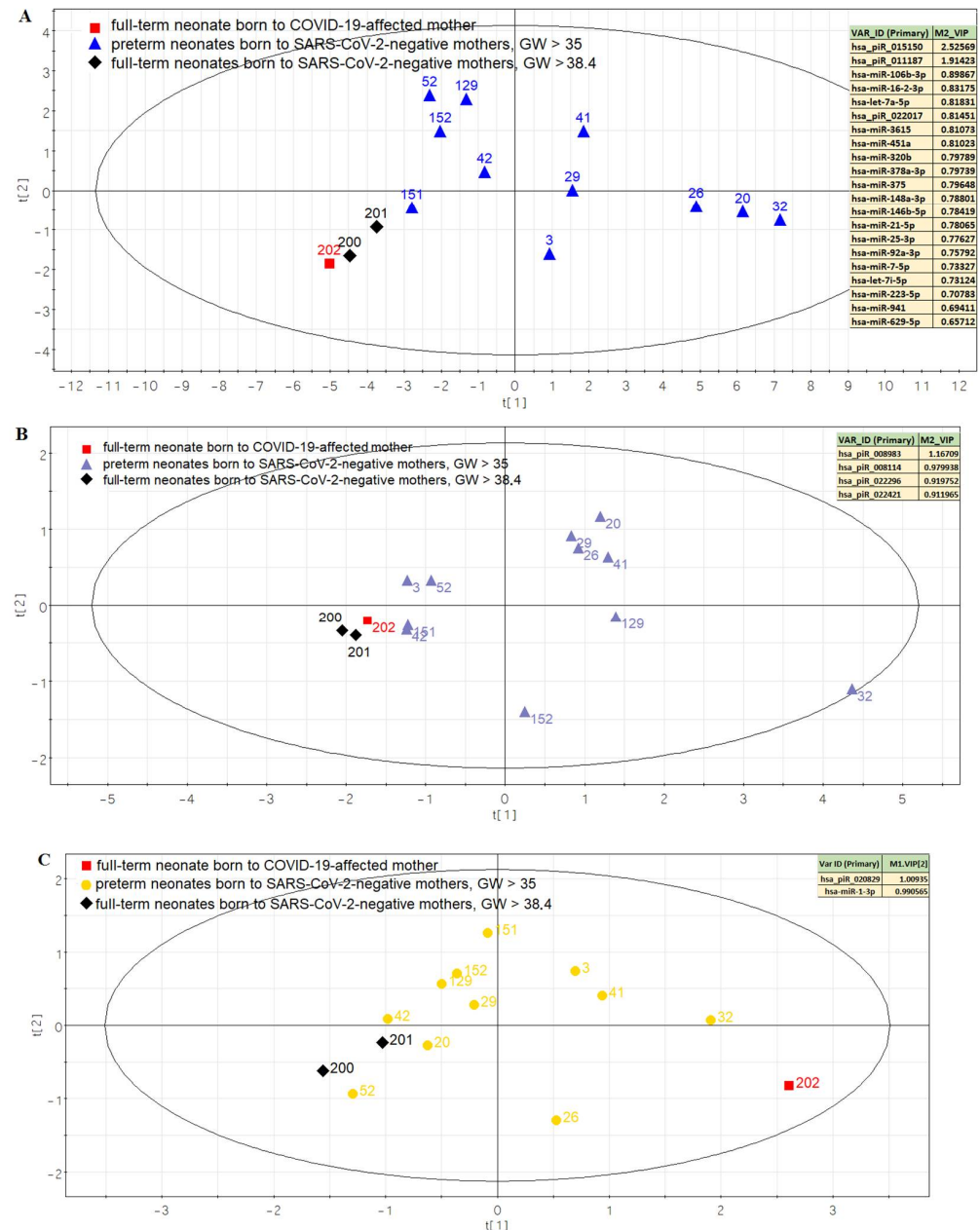


Figure 5. The score plot of the developed PLS-DA models. Changes in the circulating sncRNAs in the fetus born to the COVID-19-affected mother pre-immunized with Gam-COVID-Vac (Sputnik V) vaccine and in the newborns with severe cardiovascular and/or nervous system abnormalities are multidirectional (A), are unidirectional with more pronounced changes in the newborns with severe cardiovascular and/or nervous system abnormalities (B), are unidirectional with more pronounced changes in the fetus born to COVID-19-affected mother pre-immunized with Gam-COVID-Vac (Sputnik V) vaccine (C) relative to control samples (## 200, 201). Variable Importance in Projection (VIP) score for each RNA is presented as an insert to the right of the plot.

Table 5. miRNA and piRNA read counts according to RNA deep sequencing.

Sample ID	#3	#20	#26	#29	#32	#41	#42	#52	#129	#151	#152	#200	#201	#202
for plotting Figure 5A														
<i>hsa_piR_015150</i>	27,6414	644,966	184,276	460,690	92,138	921,380	737,104	1,382,070	737,104	460,690	921,380	92,138	368,552	0
<i>hsa_piR_011187</i>	70,008	233,360	560,064	280,032	280,032	350,040	256,696	373,376	466,720	140,016	280,032	23,336	93,344	0
<i>hsa-miR-106b-3p</i>	913	2813	2575	720	1658	804	482	51	55	94	91	63	84	20
<i>hsa-miR-16-2-3p</i>	1221	3140	2491	786	1312	874	541	70	99	196	142	113	110	34
<i>hsa-let-7a-5p</i>	3955	8260	5473	3807	7708	3504	2895	1307	744	1841	1306	849	1461	358
<i>hsa_piR_022017</i>	666	6768	3078	3474	5652	2754	810	1404	5994	486	1512	126	144	72
<i>hsa-miR-3615</i>	1942	3143	1861	679	2113	1670	674	118	99	235	136	111	140	48
<i>hsa-miR-451a</i>	14,247	23,142	21,306	6171	16,382	11,144	6930	2896	2411	5300	2263	2223	4132	1262
<i>hsa-miR-320b</i>	532	897	1415	848	2085	625	390	112	42	180	80	42	170	22
<i>hsa-miR-378a-3p</i>	400	692	738	220	604	358	246	129	62	201	122	79	75	19
<i>hsa-miR-375</i>	495	1267	2000	1805	3813	249	114	202	26	162	55	26	376	4
<i>hsa-miR-148a-3p</i>	14,673	20,316	19,939	14,605	31,354	12,062	7634	1597	972	7224	2351	1033	1954	317
<i>hsa-miR-146b-5p</i>	204	146	221	172	281	113	78	56	34	85	47	39	56	5
<i>hsa-miR-21-5p</i>	1153	1573	2033	1765	2347	1043	640	225	157	335	235	202	252	51
<i>hsa-miR-25-3p</i>	5693	8269	11,923	4326	6966	4458	2669	680	595	1656	1399	621	844	248
<i>hsa-miR-92a-3p</i>	68,340	82,079	87,803	52,288	47,904	60,556	38,042	5127	5801	12,570	12,457	5309	10,097	2946
<i>hsa-miR-7-5p</i>	1020	1384	650	828	670	614	556	50	90	162	126	64	84	20
<i>hsa-let-7i-5p</i>	5480	12,349	4463	7444	7627	5115	4832	921	1176	1819	1942	1002	1665	544
<i>hsa-miR-223-5p</i>	78	92	183	66	216	125	99	42	23	62	46	47	54	5
<i>hsa-miR-941</i>	3200	3025	1355	1530	2155	1095	660	100	75	255	185	95	95	45
<i>hsa-miR-629-5p</i>	446	944	1	256	610	178	217	55	29	58	74	58	65	13
for plotting Figure 5B														
<i>hsa_piR_008983</i>	63,472	222,152	142,812	174,548	174,548	190,416	31,736	79,340	142,812	31,736	0	0	0	15,868
<i>hsa_piR_008114</i>	2122	3697	6787	4682	9581	4029	1451	2104	4361	1803	4891	507	1288	1199
<i>hsa_piR_022296</i>	212,180	2,302,153	1,527,696	2,121,800	7,500,563	2,790,167	859,329	551,668	3,691,932	774,457	3,066,001	21,218	127,308	137,917
<i>hsa_piR_022421</i>	210	6160	3955	3885	18,270	7630	2450	1470	9310	2065	7875	175	280	560
for plotting Figure 5C														
<i>hsa_piR_020829</i>	106	55	58	76	118	104	55	26	76	100	82	27	47	114
<i>hsa-miR-1-3p</i>	18	14	44	12	44	26	4	14	4	0	4	6	8	66

The different location of samples ## 3, 20, 26, 29, 41, 42, 52, 129, 151, and 152 relative to control samples ## 200 and 201 in the PLS-DA models (Figure 5A,B) may reflect a difference in the severity of structural changes in the heart and brain of fetuses, with less pronounced changes in the fetus born of a COVID-19-affected mother (sample #202). Perhaps it was the maternal vaccination against SARS-CoV-2 prior to pregnancy that contributed to adequate humoral and cellular immunity, which protected the mother and fetus from direct (in the case of the mother) and indirect (in the case of the fetus) exposure to SARS-CoV-2 infection on the 22nd week of pregnancy. This immunization led to a mild course of COVID-19 in the mother. The fetus had lost echographic signs of right ventricular hypertrophy and hydropericardium by birth, but two small cysts (4.8 mm and 2.4 mm) in the vascular plexus were formed, probably due to a hemorrhage in this area or ischemia (impaired blood and oxygen supply) of this region.

Using the miRWalk database (http://mirwalk.umm.uni-heidelberg.de/search_mirnas/, last accessed on 1 February 2022), the functional significance of the identified 19 miRNAs was assessed (Table 5). The involvement of 13 of 19 miRNAs in the pathogenesis of cardiovascular and cerebrovascular disease, and 4 of 19 miRNAs in cardiovascular disease was identified (Figure 6). The role of miR-1-3p and miR-375 in the pathogenesis of cardiovascular disease has also been proven [51–54]. It is important to note that miR-1-3p contributed the most to sample separation in the PLS-DA model presented in Figure 5C due to its elevated expression level in the blood plasma of the newborn from the COVID-19-affected mother compared to all other samples, including controls. One of the miR-1-3p target genes is annexin A2 (ANXA2), an endothelial cell receptor for tissue-type plasminogen activator (tPA) and plasminogen, which localizes plasmin generation on the cell surface [55]. The expression level of ANXA2 determines the fibrinolytic balance in the endothelium of blood vessels [56]. Complete ANXA2 deficiency in mice has been shown to be associated with accumulation of microvascular fibrin and impaired clearance of injury-induced arterial thrombi [57]. In our recent study [58], we demonstrated for the first time a significant increase in the ratio of miR-1-3p/ANXA2 expression levels due to an increase in miR-1-3p expression and a decrease in annexin A2 expression in placental bed in a group of women with early IUGR. It can explain increased pulsatility index of uterine and umbilical arteries as a result of microvascular fibrin accumulation and, as a consequence, increased thrombogenesis, necessitating immediate pregnancy termination. The dysbalance in the homeostatic control of plasmin activity in COVID-19 patients has been demonstrated [59,60]. Moreover, the elevated serum level of miR-1-3p has been proposed as a specific biomarker for early detection of hepatocellular injury, which was more specific than traditional biomarkers such as ALT and AST [61]. Within this context, there may be a relationship between increased values of direct and total bilirubin, ALT, AST, and LDG (Table 2) and an increased level of miR-1-3p expression (Table 5) in the blood of the fetus on the first day born to COVID-19-affected mother, which may reflect hepatocellular injury as a sequence of maternal SARS-CoV-2 infection. It is important to note that the mother of the newborn also had an increase in liver transaminases because of the mild form of COVID-19.

In order to predict the possible targets of piRNAs, we used the GRCh38 database to download RefSeq transcript sequences (<https://www.ncbi.nlm.nih.gov/genome/guide/human/>, last accessed on 15 February 2022) and the miRanda algorithm with the alignment score of $sc \geq 170$ and binding energy of $en \leq -20.0$ kcal/mol, as described in our recent manuscript [62]. The list of target RNAs for these piRNAs is presented in Table S2 (Sheet 1). RefSeq mRNA accessions were converted to gene symbols using the bioDBnet database (<https://biodbnet-abcc.ncifcrf.gov/db/db2db.php>, last accessed on 15 February 2022), and this information is presented in Table S2 (Sheet 2). Using FunRich (<http://www.funrich.org/> (accessed on 15 February 2022), the possible functions of piRNA target genes and their involvement in the regulation of the cerebrovascular and cardiovascular systems was found (Table S2, Sheet 3 and Sheet 4; Figure 7).

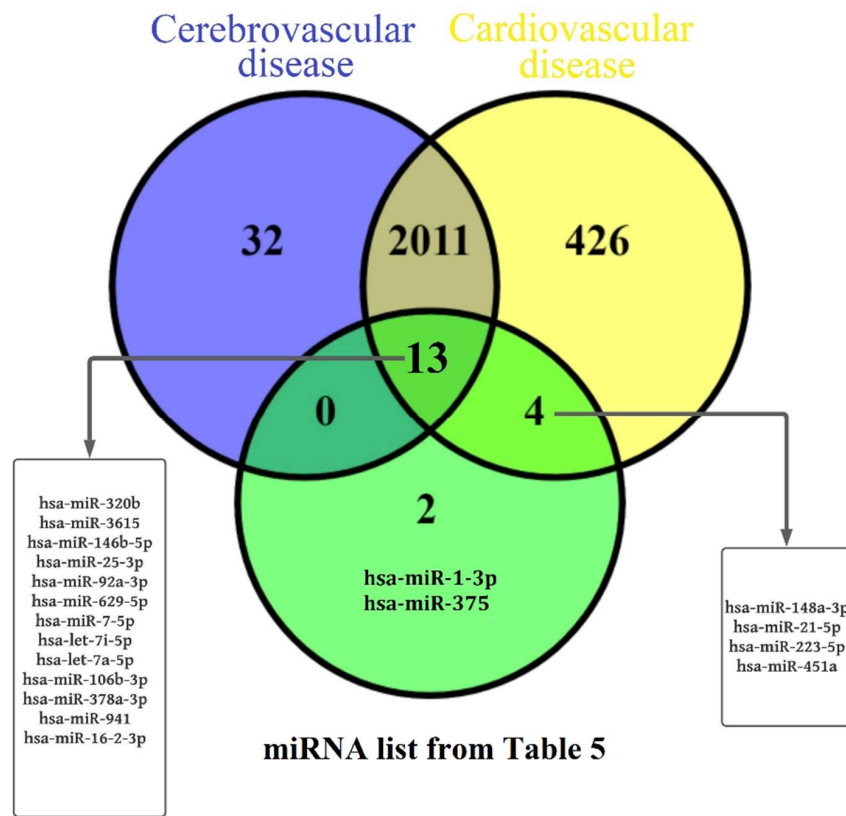


Figure 6. Venn diagram of miRNAs implicated in cerebrovascular and cardiovascular diseases according to miRWalk database, and miRNAs indicated in Table 5.

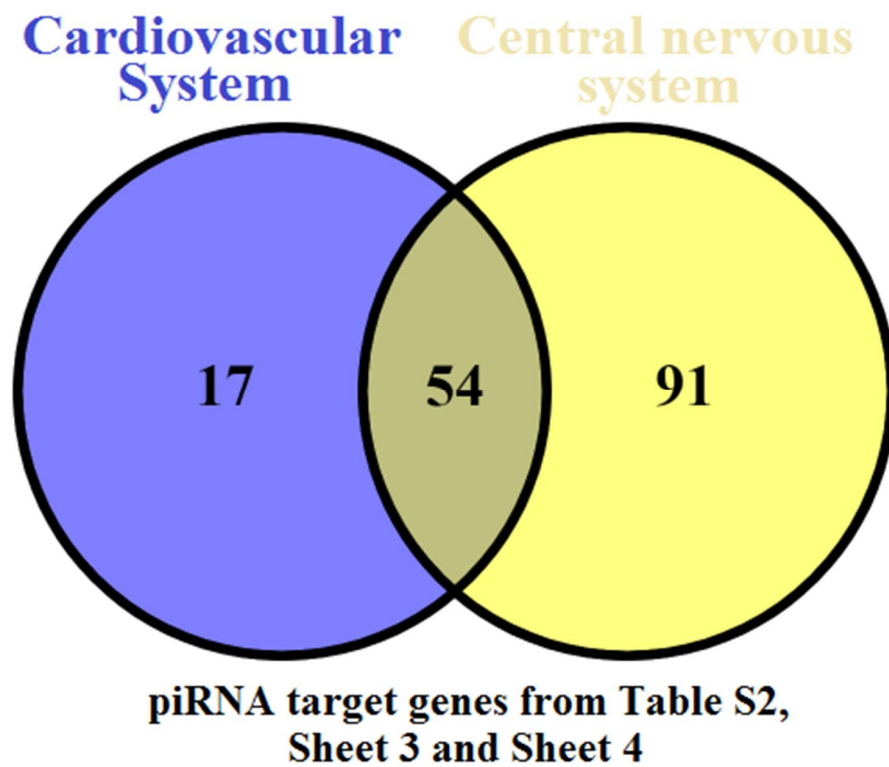


Figure 7. Venn diagram of potential piRNAs target genes involved in the regulation of the cerebrovascular and cardiovascular systems according to FunRich considering 2697 gene-targets.

4. Discussion

In the present study, we analyzed the expression profile of sncRNAs in the blood plasma of a 1-day-fetus born to a mother with SARS-CoV-2 exposure. It was of interest to find out whether maternal pre-vaccination against SARS-CoV-2 had a protective effect on the fetus and whether the profile of regulatory RNA molecules circulating in fetal blood differed from that in the blood of healthy fetuses born to mothers who were not vaccinated and never exposed to SARS-CoV-2.

Since the expression profiles in the compared samples differed, it was important to identify a possible association between changes in the expression level of sncRNAs in the newborn's plasma from a COVID-19-recovered mother and disorders in the functioning of fetal organs and systems. Taking into consideration the revealed ultrasound signs of right heart hypertrophy and hydropericardium 4 weeks after maternal exposure to SARS-CoV-2 at 22 GW, and cerebral vascular plexus cysts by the time of birth, we decided to investigate whether the expression profile of the identified sncRNAs is similar to that in neonates with more severe neonatal cardiovascular and nervous system disorders. We found that the fetus born to a SARS-CoV-2 vaccinated but COVID-19-affected woman differed from newborns with severe cardiovascular and/or nervous system abnormalities either by multidirectional changes in the circulating sncRNAs or by less pronounced unidirectional changes in the level of sncRNAs relative to control samples. In light of this, it can be concluded that vaccination against SARS-CoV-2 has a protective effect in preventing the development of pathological processes in the cardiovascular and nervous systems.

Antibodies against SARS-CoV-2 are important components in the immune response, the most important of which are IgG antibodies that target the S protein of the virus. High levels of circulating SARS-CoV-2-specific IgG detected in the serum of the 1st-day neonate in the present study could provide protective immunity transferred from its mother antenatally through the transplacental barrier. In a study of transplacental transfer of antibodies to SARS-CoV-2 in a cohort of 1471 mother–newborn dyads, Flannery and colleagues [63] showed efficient transplacental transfer of IgG antibodies in 87% of seropositive mothers.

One important indication of SARS-CoV-2 infection in severe cases is lymphopenia and neutrophilia in peripheral blood. A notable decrease in the absolute count of peripheral CD3+, CD3+CD4+, CD3+CD8+, T lymphocytes expressing activation marker HLA-DR (CD3+HLA-DR+), NK cells have been observed in patients with severe COVID-19 infection [64,65]. Our study revealed changes in the immune profile in the neonate born to a mother preliminarily vaccinated to and infected with SARS-CoV-2, in particular, increased relative count of CD3+CD4+ T cells, increased ratio of CD3+CD4+ and CD3+CD8+ T cells, increased absolute count of CD3+CD25+ T cells with receptors to IL-2, decreased absolute and relative counts of CD3+HLA-Dr., decreased relative counts of CD19+ B cells and CD19+CD5+ B1 cells, and decreased absolute and relative counts of CD3-CD16+CD56+ natural killer cells. It was shown that maternal SARS-CoV-2 infection affected neonatal immune cells and their ability to produce cytokines upon stimulation [66]. The percentage of CD4+, CD8+, NK, NK T, or $\gamma\delta$ T cells that produce TNF, IFN- γ , or IL-17 was significantly higher in neonates born to mothers exposed to SARS-CoV-2, in particular, those born to mothers with recent or ongoing infection and born to recovered mothers compared to those born to uninfected mothers. A significant increase in the percentage of CD8+ T cells expressing CD161 was found in neonates born to mothers with recent or ongoing infection but was equivalent between neonates born to recovered and uninfected mothers that compares favorably to data reported here on normal absolute and relative counts of CD3+CD8+ cells in the neonate born at 39.2 GW to a mother with the onset of COVID19 at 22 GW. The decrease in the percentages of NK cells in the newborn observed in the present study after a long period of time from the moment of infection of the mother with SARS-CoV-2 to delivery (17.2 weeks) is in good agreement with the data of Gee S. and colleagues [66] on a negative correlation of an increased percentages of NK cells in neonates born to mothers with recent or ongoing COVID-19 with number of days from a positive SARS-CoV-2 swab result to birth.

Found here was an increased relative count of CD3+ T lymphocytes with a preponderance of absolute and relative counts of CD4+ T helper cells over those of CD8+ cytotoxic T lymphocytes, and decreased relative count of CD19+ B cells, including CD19+CD5+ B1 cells, in the neonate born to the SARS-CoV-2-exposed mother indicate the predominance of T cell immunity in the newborn. CD4+ T helpers are known to play a central role in the regulation of innate and adaptive immune responses, including their activation, coordination, and modulation [67]. The increase in the absolute number of CD3+CD25+ T cells with receptors to IL-2 found here indicates the presence of an activated fraction of CD3+ T-lymphocytes and may reflect some accelerated maturation of the neonatal immune system induced in utero by maternal SARS-CoV-2 infection, since it is known that in the first year of life of newborns, T cells are immature and cellular immunity is not very competent [68]. IL-2 plays fundamental role in the differentiation of naïve CD4+ T cells into memory precursor cells followed by long-lived memory CD4+ T cell development [69–71]. In neonates born to mothers exposed to SARS-CoV-2, effector memory CD4+ T cells were significantly correlated with enhanced cytokine functionality (TNF and IFN- γ) in CD4+ T cells [66] that confirm fetal immune imprinting related to maternal SARS-CoV-2 infection.

In utero exposure to maternal inflammation associated with SARS-CoV-2 infection is recognized to affect multiple systems of the fetal organism [72]. Cord plasma of neonates born to mothers with recent or ongoing SARS-CoV-2 infection expressed elevated concentrations of cytokines IP-10, IL-10, and CXCL8 [66] known to be associated with adult SARS-CoV-2 infection [65,73] and found to be of maternal origin by their transfer through the placental tissues and/or be of neonatal origin as a direct response to maternal SARS-CoV-2 infection. There was a relationship between fetal proinflammatory cytokine levels and maternal infection status at the time of birth, with less obvious changes in neonates born to mothers with recovered infection. Such neonatal blood plasma inflammation profile is consistent with transcriptional changes in placentas from individuals with COVID-19 [74]. Even in the absence of placental SARS-CoV-2 RNA, placental transcriptome analysis showed increased expression of genes encoding cytotoxic proteins, chemokines, and proinflammatory proteins. Among the overexpressed genes, HSPA1A, which has been found to be involved in placental vascular diseases and preeclampsia, has changed most significantly [75]. Histological analysis of the placenta of the woman who recovered from COVID19 in the present study revealed predominance of angiogenesis with branching of vessels and increased fetal fibrinoid deposition in the decidual plate. Increased intervillous fibrinous deposits are often found in placental tissues in pregnant women with SARS-CoV-2 infection, but not in any of the control placentas [74,76]. An abnormal immune reaction has been proposed as the cause of extensive perivillous fibrin depositions and chronic intervillitis [23,77]. The predominance of angiogenesis with branching vessels in the placenta of COVID-19-affected women revealed by us can be considered as a compensatory process to increase the area of gas exchange of the villous tree in response to uteroplacental hypoxia caused by maternal SARS-CoV-2 infection, as has been demonstrated in preeclampsia [78]. The key role in the formation of fetoplacental angiogenesis throughout gestation is assigned to the vascular endothelial growth factor (VEGF) and its receptors (VEGFR-1 and VEGFR-2), placental growth factor (PlGF), angiopoietins, and many other growth factors, which are upregulated with low oxygen tension to facilitate the expansion of placental vascular network [79]. Normal development of the human placenta is characterized by branching angiogenesis (the formation of new vessels by sprouting) up to 24 GW, followed by nonbranching angiogenesis (the formation of capillary loops through elongation) up to term. Therefore, the predominance of branched over unbranched angiogenesis as in the clinical case presented in the present study reflects posthypoxic pathological processes in the placenta.

In summary, we identified a first day newborn's blood plasma sncRNA profile associated with cardiovascular and nervous system disorders. Moreover, in comparison with a newborn without perinatal complications, this sncRNA profile was changed to a lesser extent in a neonate born to a COVID-19-affected mother pre-immunized with

Gam-COVID-Vac (Sputnik V) vaccine than in the neonates with severe cardiovascular or central nervous system disorders. We would like to emphasize that all the above suggests mild antenatal exposure of the fetus to maternal COVID-19, namely normalization of echocardiographic parameters and detection of two cysts of the cerebral plexus at birth without neurological symptoms as well as a slight change in the immunogram with a predominance of T-cell immunity, which is likely due to maternal immunization against SARS-CoV-2 prior to pregnancy and the presence of anti-SARS-CoV-2 IgG antibodies in mother and fetus. This clinical pattern is quite different from that presented in the article of Kappanayil M. and colleagues [72], describing severe hyperinflammatory syndrome in a neonate with myocarditis, hepatomegaly, shock, substantial elevation of cardiac markers (N-terminal-pro-B-type natriuretic peptide, myocardial creatine kinase, troponin T), elevation of hepatic transaminases (aspartate aminotransferase, alanine aminotransferase), inflammatory markers (serum ferritin and lactate dehydrogenase, C-reactive protein), and multiorgan dysfunction following proven prenatal exposure to mild COVID-19 at 31 GW in the absence of prior vaccination of the mother against SARS-CoV-2. Lack of prior vaccination of the mother against SARS-CoV-2 and maternal illness with COVID-19 at 21 weeks of gestation also led to severe antenatal complications, in particular, critical blood flow in the fetal umbilical artery, fetal growth restriction (1st percentile), right ventricular hypertrophy, hydropericardium, echo-characteristics of hypoxic-ischemic brain injury (leukomalacia in periventricular area), intraventricular hemorrhage, which resulted in the neonate death at the 26th week of gestation [80]. These two cases in comparison with the clinical and molecular biological pattern in the neonate described in the present study highlight the importance of vaccination against SARS-CoV-2 before pregnancy.

5. Conclusions

We can conclude the protective effect of SARS-CoV-2 vaccination in preventing the progression of pathological processes in the cardiovascular and nervous systems of the fetus under exposure of maternal SARS-CoV-2 infection. However, careful postnatal observation and examination of newborns from COVID-19-recovered mothers is necessary, because we found increased levels of circulating miR-1-3p in the first-day newborn, which is not only a marker of liver cell damage [61], but also can cause fibrin accumulation and impaired clearance of injury-induced arterial thrombi being the regulator of the expression level of its target gene ANXA2 (the endothelial cell receptor for tissue-type plasminogen activator (tPA) and plasminogen) [58].

With this study, we would like to emphasize the importance of evaluating the efficacy and safety of vaccination at the molecular level, since the lack of adequate information about vaccines already available or under development has been reported as one of the main drivers of hesitancy towards anti-SARS-CoV2 vaccination primarily among healthcare workers [81], playing a key role in spreading information about vaccine and patient guidance. In order to develop protocols for the management of pregnant women, we propose to evaluate the efficacy and safety of available vaccines while applying Omics technologies for the investigation of the peripheral blood of mother and newborn with the formation of groups for comparison depending on (i) the time of vaccination (before pregnancy or in different trimesters of pregnancy), (ii) the time period from the vaccination to the onset of COVID-19, (iii) the severity of maternal COVID-19, (iv) maternal anti-SARS-CoV2 antibodies titer after vaccination and after onset of COVID-19, (v) neonatal anti-SARS-CoV2 antibodies titer at the time of birth, and (vi) neonatal period characteristics in comparison with that in the absence of maternal vaccination.

Supplementary Materials: The following supporting information can be downloaded at <https://www.mdpi.com/article/10.3390/covid2070061/s1>. Table S1: Detailed clinical characteristics of newborns and their mothers; Table S2: Potential mRNA targets of piRNA and their function.

Author Contributions: Conceptualization, A.V.T. and V.V.Z.; methodology, A.V.T.; software, V.V.C.; validation, A.V.T., and I.S.F.; formal analysis, V.V.Z.; investigation, A.V.T.; resources, V.V.Z.; data curation, V.E.F.; writing—Original draft preparation, A.V.T.; writing—Review and editing, A.V.T.; visualization, I.S.F., M.I.M., and A.B.S.; supervision, V.E.F.; project administration, G.T.S.; funding acquisition, V.E.F. and G.T.S. All authors have read and agreed to the published version of the manuscript.

Funding: This research was funded by RFBR according to the research project № 20-04-60093.

Institutional Review Board Statement: The study was conducted according to the guidelines of the Declaration of Helsinki and approved by the ethics committee of the National Medical Research Center for Obstetrics, Gynecology, and Perinatology, named after Academician V.I. Kulakov of Ministry of Healthcare of the Russian Federation (ethics committee approval protocol No 4, approval date: 23 April 2020; ethics committee approval protocol No 11, approval date: 11 November 2021).

Informed Consent Statement: Informed consent was obtained from all subjects involved in the study.

Data Availability Statement: Not applicable.

Acknowledgments: The authors of the article are grateful to Shchegolev Alexander Ivanovich, from the second pathoanatomical department of FSBI “National Medical Research Center for Obstetrics, Gynecology, and Perinatology, named after Academician V.I. Kulakov” Ministry of Healthcare of the Russian Federation, for providing illustrative material on the histological analysis of the placenta.

Conflicts of Interest: The authors declare no conflict of interest. The funders had no role in the design of the study; in the collection, analyses, or interpretation of data; in the writing of the manuscript, or in the decision to publish the results.

References

1. Cascella, M.; Rajnik, M.; Cuomo, A.; Dulebohn, S.C.; Di Napoli, R. Features, Evaluation and Treatment Coronavirus (COVID-19). In *StatPearls*; StatPearls Publishing: Treasure Island, FL, USA, 2020.
2. Bahadur, G.; Bhat, M.; Acharya, S.; Janga, D.; Cambell, B.; Huirne, J.; Yoong, W.; Govind, A.; Pardo, J.; Homburg, R. Retrospective observational RT-PCR analyses on 688 babies born to 843 SARS-CoV-2 positive mothers, placental analyses and diagnostic analyses limitations suggest vertical transmission is possible. *Facts Views Vis. ObGyn* **2021**, *13*, 53–66. [[CrossRef](#)] [[PubMed](#)]
3. Gajbhiye, R.K.; Modi, D.N.; Mahale, S.D. Pregnancy outcomes, Newborn complications and Maternal-Fetal Transmission of SARS-CoV-2 in women with COVID-19: A systematic review of 441 cases. *medRxiv* **2020**. medRxiv:2020.04.11.20062356. [[CrossRef](#)]
4. Lamouroux, A.; Attie-Bitach, T.; Martinovic, J.; Leruez-Ville, M.; Ville, Y. Evidence for and against vertical transmission for severe acute respiratory syndrome coronavirus 2. *Am. J. Obstet. Gynecol.* **2020**, *223*, 91.e1–91.e4. [[CrossRef](#)] [[PubMed](#)]
5. Kotlyar, A.M.; Grechukhina, O.; Chen, A.; Popkhadze, S.; Grimshaw, A.; Tal, O.; Taylor, H.S.; Tal, R. Vertical transmission of coronavirus disease 2019: A systematic review and meta-analysis. *Am. J. Obstet. Gynecol.* **2021**, *224*, 35–53.e3. [[CrossRef](#)]
6. Wong, Y.P.; Khong, T.Y.; Tan, G.C. The Effects of COVID-19 on Placenta and Pregnancy: What Do We Know So Far? *Diagnostics* **2021**, *11*, 94. [[CrossRef](#)]
7. Kreis, N.-N.; Ritter, A.; Louwen, F.; Yuan, J. A Message from the Human Placenta: Structural and Immunomodulatory Defense against SARS-CoV-2. *Cells* **2020**, *9*, 1777. [[CrossRef](#)]
8. Burton, G.J.; Fowden, A.L. The placenta: A multifaceted, transient organ. *Philos. Trans. R. Soc. B Biol. Sci.* **2015**, *370*, 20140066. [[CrossRef](#)]
9. Celik, O.; Saglam, A.; Baysal, B.; Derwig, I.E.; Celik, N.; Ak, M.; Aslan, S.N.; Ulas, M.; Ersahin, A.; Tayyar, A.T.; et al. Factors preventing materno-fetal transmission of SARS-CoV-2. *Placenta* **2020**, *97*, 1–5. [[CrossRef](#)]
10. Li, M.; Chen, L.; Zhang, J.; Xiong, C.; Li, X. The SARS-CoV-2 receptor ACE2 expression of maternal-fetal interface and fetal organs by single-cell transcriptome study. *PLoS ONE* **2020**, *15*, e0230295. [[CrossRef](#)]
11. Roopenian, D.C.; Akilesh, S. FcRn: The neonatal Fc receptor comes of age. *Nat. Rev. Immunol.* **2007**, *7*, 715–725. [[CrossRef](#)]
12. Maltepe, E.; Fisher, S.J. Placenta: The Forgotten Organ. *Annu. Rev. Cell Dev. Biol.* **2015**, *31*, 523–552. [[CrossRef](#)] [[PubMed](#)]
13. Robbins, J.R.; Bakardjiev, A.I. Pathogens and the placental fortress. *Curr. Opin. Microbiol.* **2012**, *15*, 36–43. [[CrossRef](#)] [[PubMed](#)]
14. Heerema-McKenney, A. Defense and infection of the human placenta. *APMIS* **2018**, *126*, 570–588. [[CrossRef](#)] [[PubMed](#)]
15. Pique-Regi, R.; Romero, R.; Tarca, A.L.; Luca, F.; Xu, Y.; Alazizi, A.; Leng, Y.; Hsu, C.-D.; Gomez-Lopez, N. Does the human placenta express the canonical cell entry mediators for SARS-CoV-2? *Elife* **2020**, *9*, e58716. [[CrossRef](#)]
16. Tan, C.; Li, S.; Liang, Y.; Chen, M.; Liu, J. SARS-CoV-2 viremia may predict rapid deterioration of COVID-19 patients. *Braz. J. Infect. Dis.* **2020**, *24*, 565–569. [[CrossRef](#)]
17. Sathiya, R.; Rajendran, J.; Sumathi, S. COVID-19 and Preeclampsia: Overlapping Features in Pregnancy. *Rambam Maimonides Med. J.* **2022**, *13*, e0007. [[CrossRef](#)]

18. Liu, P.; Zheng, J.; Yang, P.; Wang, X.; Wei, C.; Zhang, S.; Feng, S.; Lan, J.; He, B.; Zhao, D.; et al. The immunologic status of newborns born to SARS-CoV-2-infected mothers in Wuhan, China. *J. Allergy Clin. Immunol.* **2020**, *146*, 101–109.e1. [[CrossRef](#)]
19. Vimercati, A.; De Nola, R.; Trerotoli, P.; Metta, M.E.; Cazzato, G.; Resta, L.; Malvasi, A.; Lepera, A.; Ricci, I.; Capozza, M.; et al. COVID-19 Infection in Pregnancy: Obstetrical Risk Factors and Neonatal Outcomes-A Monocentric, Single-Cohort Study. *Vaccines* **2022**, *10*, 166. [[CrossRef](#)]
20. Joma, M.; Fovet, C.-M.; Seddiki, N.; Gressens, P.; Laforge, M. COVID-19 and Pregnancy: Vertical Transmission and Inflammation Impact on Newborns. *Vaccines* **2021**, *9*, 391. [[CrossRef](#)]
21. Schoenmakers, S.; Sniijder, P.; Verdijk, R.M.; Kuiken, T.; Kamphuis, S.S.M.; Koopman, L.P.; Krasemann, T.B.; Rousian, M.; Broekhuizen, M.; Steegers, E.A.P.; et al. Severe Acute Respiratory Syndrome Coronavirus 2 Placental Infection and Inflammation Leading to Fetal Distress and Neonatal Multi-Organ Failure in an Asymptomatic Woman. *J. Pediatr. Infect. Dis. Soc.* **2021**, *10*, 556–561. [[CrossRef](#)]
22. Correia, C.R.; Marçal, M.; Vieira, F.; Santos, E.; Novais, C.; Maria, A.T.; Malveiro, D.; Prior, A.R.; Aguiar, M.; Salazar, A.; et al. Congenital SARS-CoV-2 Infection in a Neonate With Severe Acute Respiratory Syndrome. *Pediatr. Infect. Dis. J.* **2020**, *39*, e439–e443. [[CrossRef](#)] [[PubMed](#)]
23. Vivanti, A.J.; Vauloup-Fellous, C.; Prevot, S.; Zupan, V.; Suffee, C.; Do Cao, J.; Benachi, A.; De Luca, D. Transplacental transmission of SARS-CoV-2 infection. *Nat. Commun.* **2020**, *11*, 3572. [[CrossRef](#)] [[PubMed](#)]
24. Di Nicola, P.; Ceratto, S.; Dalmazzo, C.; Roasio, L.; Castagnola, E.; Sannia, A. Concomitant SARS-CoV-2 infection and severe neurologic involvement in a late-preterm neonate. *Neurology* **2020**, *95*, 834–835. [[CrossRef](#)] [[PubMed](#)]
25. Favre, G.; Mazzetti, S.; Gengler, C.; Bertelli, C.; Schneider, J.; Laubscher, B.; Capoccia, R.; Pakniyat, F.; Ben Jazia, I.; Eggel-Hort, B.; et al. Decreased Fetal Movements: A Sign of Placental SARS-CoV-2 Infection with Perinatal Brain Injury. *Viruses* **2021**, *13*, 2517. [[CrossRef](#)]
26. Gale, C.; Quigley, M.A.; Placzek, A.; Knight, M.; Ladhani, S.; Draper, E.S.; Sharkey, D.; Doherty, C.; Mactier, H.; Kurinczuk, J.J. Characteristics and outcomes of neonatal SARS-CoV-2 infection in the UK: A prospective national cohort study using active surveillance. *Lancet Child Adolesc. Health* **2021**, *5*, 113–121. [[CrossRef](#)]
27. Yoon, S.H.; Kang, J.-M.; Ahn, J.G. Clinical outcomes of 201 neonates born to mothers with COVID-19: A systematic review. *Eur. Rev. Med. Pharmacol. Sci.* **2020**, *24*, 7804–7815. [[CrossRef](#)]
28. Di Girolamo, R.; Khalil, A.; Alameddine, S.; D’Angelo, E.; Galliani, C.; Matarrelli, B.; Buca, D.; Liberati, M.; Rizzo, G.; D’Antonio, F. Placental histopathology after SARS-CoV-2 infection in pregnancy: A systematic review and meta-analysis. *Am. J. Obstet. Gynecol. MFM* **2021**, *3*, 100468. [[CrossRef](#)]
29. Resta, L.; Vimercati, A.; Cazzato, G.; Mazzia, G.; Cicinelli, E.; Colagrande, A.; Fanelli, M.; Scarcella, S.V.; Ceci, O.; Rossi, R. SARS-CoV-2 and Placenta: New Insights and Perspectives. *Viruses* **2021**, *13*, 723. [[CrossRef](#)]
30. Cribiù, F.M.; Erra, R.; Pagni, L.; Rubio-Perez, C.; Alonso, L.; Simonetti, S.; Croci, G.A.; Serna, G.; Ronchi, A.; Pietrasanta, C.; et al. Severe SARS-CoV-2 placenta infection can impact neonatal outcome in the absence of vertical transmission. *J. Clin. Investig.* **2021**, *131*, e145427. [[CrossRef](#)]
31. Resta, L.; Vimercati, A.; Sablone, S.; Marzullo, A.; Cazzato, G.; Ingravallo, G.; Mazzia, G.; Arezzo, F.; Colagrande, A.; Rossi, R. Is the First of the Two Born Saved? A Rare and Dramatic Case of Double Placental Damage from SARS-CoV-2. *Viruses* **2021**, *13*, 995. [[CrossRef](#)]
32. Kontou, A.; Virgiliou, C.; Mouskeftara, T.; Begou, O.; Meikopoulos, T.; Thomaidou, A.; Agakidou, E.; Gika, H.; Theodoridis, G.; Sarafidis, K. Plasma Lipidomic and Metabolomic Profiling after Birth in Neonates Born to SARS-CoV-19 Infected and Non-Infected Mothers at Delivery: Preliminary Results. *Metabolites* **2021**, *11*, 830. [[CrossRef](#)] [[PubMed](#)]
33. Cai, A.; Hu, Y.; Zhou, Z.; Qi, Q.; Wu, Y.; Dong, P.; Chen, L.; Wang, F. PIWI-Interacting RNAs (piRNAs): Promising Applications as Emerging Biomarkers for Digestive System Cancer. *Front. Mol. Biosci.* **2022**, *9*, 848105. [[CrossRef](#)] [[PubMed](#)]
34. Deogharia, M.; Gurha, P. The “guiding” principles of noncoding RNA function. *Wiley Interdiscip. Rev. RNA* **2021**, e1704. [[CrossRef](#)]
35. Zhu, Q.; Kirby, J.A.; Chu, C.; Gou, L.-T. Small Noncoding RNAs in Reproduction and Infertility. *Biomed* **2021**, *9*, 1884. [[CrossRef](#)] [[PubMed](#)]
36. Santosh, B.; Varshney, A.; Yadava, P.K. Non-coding RNAs: Biological functions and applications. *Cell Biochem. Funct.* **2015**, *33*, 14–22. [[CrossRef](#)]
37. Iwakawa, H.; Tomari, Y. Life of RISC: Formation, action, and degradation of RNA-induced silencing complex. *Mol. Cell* **2022**, *82*, 30–43. [[CrossRef](#)]
38. Saulle, I.; Garziano, M.; Fenizia, C.; Cappelletti, G.; Parisi, F.; Clerici, M.; Cetin, I.; Savasi, V.; Biasin, M. MiRNA Profiling in Plasma and Placenta of SARS-CoV-2-Infected Pregnant Women. *Cells* **2021**, *10*, 1788. [[CrossRef](#)]
39. Farr, R.J.; Rootes, C.L.; Rowntree, L.C.; Nguyen, T.H.O.; Hensen, L.; Kedzierski, L.; Cheng, A.C.; Kedzierska, K.; Au, G.G.; Marsh, G.A.; et al. Altered microRNA expression in COVID-19 patients enables identification of SARS-CoV-2 infection. *PLoS Pathog.* **2021**, *17*, e1009759. [[CrossRef](#)]
40. Meidert, A.S.; Hermann, S.; Brandes, F.; Kirchner, B.; Buschmann, D.; Billaud, J.-N.; Klein, M.; Lindemann, A.; Aue, E.; Schelling, G.; et al. Extracellular Vesicle Associated miRNAs Regulate Signaling Pathways Involved in COVID-19 Pneumonia and the Progression to Severe Acute Respiratory Corona Virus-2 Syndrome. *Front. Immunol.* **2021**, *12*, 784028. [[CrossRef](#)]
41. Male, V. SARS-CoV-2 infection and COVID-19 vaccination in pregnancy. *Nat. Rev. Immunol.* **2022**, *22*, 277–282. [[CrossRef](#)]
42. Jamieson, D.J.; Rasmussen, S.A. An update on COVID-19 and pregnancy. *Am. J. Obstet. Gynecol.* **2022**, *226*, 177–186. [[CrossRef](#)]
43. Martin, M. Cutadapt removes adapter sequences from high-throughput sequencing reads. *EMBnet J.* **2011**, *17*, 10–12. [[CrossRef](#)]

44. Griffiths-Jones, S.; Grocock, R.J.; van Dongen, S.; Bateman, A.; Enright, A.J. miRBase: MicroRNA sequences, targets and gene nomenclature. *Nucleic Acids Res.* **2006**, *34*, D140–D144. [[CrossRef](#)]
45. Langmead, B.; Trapnell, C.; Pop, M.; Salzberg, S.L. Ultrafast and memory-efficient alignment of short DNA sequences to the human genome. *Genome Biol.* **2009**, *10*, R25. [[CrossRef](#)] [[PubMed](#)]
46. R Core Team. A Language and Environment for Statistical Computing. In *R Foundation for Statistical Computing*; R Core Team: Vienna, Austria, 2020; Available online: <https://www.r-project.org> (accessed on 10 March 2021).
47. Love, M.I.; Huber, W.; Anders, S. Moderated estimation of fold change and dispersion for RNA-seq data with DESeq2. *Genome Biol.* **2014**, *15*, 550. [[CrossRef](#)] [[PubMed](#)]
48. R Core Team. *RStudio: Integrated Development for R*; RStudio: Vienna, Austria, 2021; Available online: <http://www.rstudio.com/> (accessed on 23 March 2021).
49. Wold, S.; Sjöström, M.; Eriksson, L. PLS-regression: A basic tool of chemometrics. *Chemom. Intell. Lab. Syst.* **2001**, *58*, 109–130. [[CrossRef](#)]
50. Rajalahti, T.; Arneberg, R.; Kroksveen, A.C.; Berle, M.; Myhr, K.-M.; Kvalheim, O.M. Discriminating variable test and selectivity ratio plot: Quantitative tools for interpretation and variable (biomarker) selection in complex spectral or chromatographic profiles. *Anal. Chem.* **2009**, *81*, 2581–2590. [[CrossRef](#)]
51. Li, M.; Chen, X.; Chen, L.; Chen, K.; Zhou, J.; Song, J. MiR-1-3p that correlates with left ventricular function of HCM can serve as a potential target and differentiate HCM from DCM. *J. Transl. Med.* **2018**, *16*, 161. [[CrossRef](#)]
52. Kura, B.; Kalocayova, B.; Devaux, Y.; Bartekova, M. Potential Clinical Implications of miR-1 and miR-21 in Heart Disease and Cardioprotection. *Int. J. Mol. Sci.* **2020**, *21*, 700. [[CrossRef](#)]
53. Schuchardt, E.L.; Miyamoto, S.D.; Crombleholme, T.; Karimpour-Fard, A.; Korst, A.; Neltner, B.; Howley, L.W.; Cuneo, B.; Sucharov, C.C. Amniotic Fluid microRNA in Severe Twin-Twin Transfusion Syndrome Cardiomyopathy-Identification of Differences and Predicting Demise. *J. Cardiovasc. Dev. Dis.* **2022**, *9*, 37. [[CrossRef](#)]
54. Baulina, N.; Osmak, G.; Kiselev, I.; Matveeva, N.; Kukava, N.; Shakhnovich, R.; Kulakova, O.; Favorova, O. NGS-identified circulating miR-375 as a potential regulating component of myocardial infarction associated network. *J. Mol. Cell. Cardiol.* **2018**, *121*, 173–179. [[CrossRef](#)] [[PubMed](#)]
55. Cesarman, G.M.; Guevara, C.A.; Hajjar, K.A. An endothelial cell receptor for plasminogen/tissue plasminogen activator (t-PA). II. Annexin II-mediated enhancement of t-PA-dependent plasminogen activation. *J. Biol. Chem.* **1994**, *269*, 21198–21203. [[CrossRef](#)]
56. Dassah, M.; Deora, A.B.; He, K.; Hajjar, K.A. The endothelial cell annexin A2 system and vascular fibrinolysis. *Gen. Physiol. Biophys.* **2009**, *28*, F20–F28. [[PubMed](#)]
57. Ling, Q.; Jacovina, A.T.; Deora, A.; Febbraio, M.; Simantov, R.; Silverstein, R.L.; Hempstead, B.; Mark, W.H.; Hajjar, K.A. Annexin II regulates fibrin homeostasis and neoangiogenesis in vivo. *J. Clin. Investig.* **2004**, *113*, 38–48. [[CrossRef](#)]
58. Timofeeva, A.V.; Fedorov, I.S.; Brzhozovskiy, A.G.; Bugrova, A.E.; Chagovets, V.V.; Volochaeva, M.V.; Starodubtseva, N.L.; Frankevich, V.E.; Nikolaev, E.N.; Shmakov, R.G.; et al. miRNAs and Their Gene Targets-A Clue to Differentiate Pregnancies with Small for Gestational Age Newborns, Intrauterine Growth Restriction, and Preeclampsia. *Diagnostics* **2021**, *11*, 729. [[CrossRef](#)]
59. Cabrera-Garcia, D.; Miltiades, A.; Parsons, S.; Elisman, K.; Mansouri, M.T.; Wagener, G.; Harrison, N.L. High levels of plasminogen activator inhibitor-1, tissue plasminogen activator and fibrinogen in patients with severe COVID-19. *medRxiv* **2021**. medRxiv:2020.12.29.20248869. [[CrossRef](#)]
60. Rubina, K.; Shmakova, A.; Shabanov, A.; Andreev, Y.; Borovkova, N.; Kulabukhov, V.; Evseev, A.; Popugaev, K.; Petrikov, S.; Semina, E. Novel prognostic determinants of COVID-19-related mortality: A pilot study on severely-ill patients in Russia. *PLoS ONE* **2022**, *17*, e0264072. [[CrossRef](#)]
61. Kagawa, T.; Shirai, Y.; Oda, S.; Yokoi, T. Identification of Specific MicroRNA Biomarkers in Early Stages of Hepatocellular Injury, Cholestasis, and Steatosis in Rats. *Toxicol. Sci.* **2018**, *166*, 228–239. [[CrossRef](#)]
62. Timofeeva, A.; Drapkina, Y.; Fedorov, I.; Chagovets, V.; Makarova, N.; Shamina, M.; Kalinina, E.; Sukhikh, G. Small Noncoding RNA Signatures for Determining the Developmental Potential of an Embryo at the Morula Stage. *Int. J. Mol. Sci.* **2020**, *21*, 9399. [[CrossRef](#)]
63. Flannery, D.D.; Gouma, S.; Dhudasia, M.B.; Mukhopadhyay, S.; Pfeifer, M.R.; Woodford, E.C.; Triebwasser, J.E.; Gerber, J.S.; Morris, J.S.; Weirick, M.E.; et al. Assessment of Maternal and Neonatal Cord Blood SARS-CoV-2 Antibodies and Placental Transfer Ratios. *JAMA Pediatr.* **2021**, *175*, 594–600. [[CrossRef](#)]
64. Krechetova, L.V.; Inviyaeva, E.V.; Sadykov, V.F.; Vtorushina, V.V.; Ivanets, T.Y.; Silachev, D.N.; Pyregov, A.V.; Dolgushina, N.V.; Sukhikh, G.T. Immune status of covid-19 patients with different disease severity. *Akusherstvo Ginekol.* **2021**, *2021*, 75–88. [[CrossRef](#)]
65. Laing, A.G.; Lorenc, A.; Del Molino Del Barrio, I.; Das, A.; Fish, M.; Monin, L.; Muñoz-Ruiz, M.; McKenzie, D.R.; Hayday, T.S.; Francos-Quijorna, I.; et al. A dynamic COVID-19 immune signature includes associations with poor prognosis. *Nat. Med.* **2020**, *26*, 1623–1635. [[CrossRef](#)] [[PubMed](#)]
66. Gee, S.; Chandiramani, M.; Seow, J.; Pollock, E.; Modestini, C.; Das, A.; Tree, T.; Doores, K.J.; Tribe, R.M.; Gibbons, D.L. The legacy of maternal SARS-CoV-2 infection on the immunology of the neonate. *Nat. Immunol.* **2021**, *22*, 1490–1502. [[CrossRef](#)] [[PubMed](#)]
67. Raphael, I.; Joern, R.R.; Forsthuber, T.G. Memory CD4(+) T Cells in Immunity and Autoimmune Diseases. *Cells* **2020**, *9*, 531. [[CrossRef](#)]

68. Kapustova, L.; Petrovicova, O.; Banovcin, P.; Antosova, M.; Bobcakova, A.; Urbancikova, I.; Rennerova, Z.; Jesenak, M. COVID-19 and the differences in physiological background between children and adults and their clinical consequences. *Physiol. Res.* **2021**, *70*, S209–S225. [[CrossRef](#)]
69. Dhume, K.; McKinstry, K.K. Early programming and late-acting checkpoints governing the development of CD4 T-cell memory. *Immunology* **2018**, *155*, 53–62. [[CrossRef](#)]
70. Belz, G.T.; Masson, F. Interleukin-2 tickles T cell memory. *Immunity* **2010**, *32*, 7–9. [[CrossRef](#)]
71. Raeber, M.E.; Zurbuchen, Y.; Impellizzieri, D.; Boyman, O. The role of cytokines in T-cell memory in health and disease. *Immunol. Rev.* **2018**, *283*, 176–193. [[CrossRef](#)]
72. Kappanayil, M.; Balan, S.; Alawani, S.; Mohanty, S.; Leeladharan, S.P.; Gangadharan, S.; Jayashankar, J.P.; Jagadeesan, S.; Kumar, A.; Gupta, A.; et al. Multisystem inflammatory syndrome in a neonate, temporally associated with prenatal exposure to SARS-CoV-2: A case report. *Lancet Child Adolesc. Health* **2021**, *5*, 304–308. [[CrossRef](#)]
73. Arunachalam, P.S.; Wimmers, F.; Mok, C.K.P.; Perera, R.A.P.M.; Scott, M.; Hagan, T.; Sigal, N.; Feng, Y.; Bristow, L.; Tak-Yin Tsang, O.; et al. Systems biological assessment of immunity to mild versus severe COVID-19 infection in humans. *Science* **2020**, *369*, 1210–1220. [[CrossRef](#)]
74. Lu-Culligan, A.; Chavan, A.R.; Vijayakumar, P.; Irshaid, L.; Courchaine, E.M.; Milano, K.M.; Tang, Z.; Pope, S.D.; Song, E.; Vogels, C.B.F.; et al. Maternal respiratory SARS-CoV-2 infection in pregnancy is associated with a robust inflammatory response at the maternal-fetal interface. *Med* **2021**, *2*, 591–610.e10. [[CrossRef](#)] [[PubMed](#)]
75. Brien, M.-E.; Baker, B.; Duval, C.; Gaudreault, V.; Jones, R.L.; Girard, S. Alarmins at the maternal-fetal interface: Involvement of inflammation in placental dysfunction and pregnancy complications (1). *Can. J. Physiol. Pharmacol.* **2019**, *97*, 206–212. [[CrossRef](#)] [[PubMed](#)]
76. Dubucs, C.; Groussolles, M.; Ousselin, J.; Sartor, A.; Van Acker, N.; Vayssière, C.; Pasquier, C.; Reyre, J.; Batlle, L.; Favarel Clinical Research Associate, S.; et al. Severe placental lesions due to maternal SARS-CoV-2 infection associated to intrauterine fetal death. *Hum. Pathol.* **2022**, *121*, 46–55. [[CrossRef](#)] [[PubMed](#)]
77. Mongula, J.E.; Frenken, M.W.E.; van Lijnschoten, G.; Arents, N.L.A.; de Wit-Zuurendonk, L.D.; Schimmel-de Kok, A.P.A.; van Runnard Heimel, P.J.; Porath, M.M.; Goossens, S.M.T.A. COVID-19 during pregnancy: Non-reassuring fetal heart rate, placental pathology and coagulopathy. *Ultrasound Obstet. Gynecol.* **2020**, *56*, 773–776. [[CrossRef](#)]
78. Shchegolev, A.I.; Lyapin, V.M.; Tumanova, U.N.; Vodneva, D.N.; Shmakov, R.G. Histological changes in the placenta and vascularization of its villi in early-And lateonset Preeclampsia. *Arkh. Patol.* **2016**, *78*, 13–18. [[CrossRef](#)]
79. Chen, D.-B.; Zheng, J. Regulation of placental angiogenesis. *Microcirculation* **2014**, *21*, 15–25. [[CrossRef](#)]
80. Sukhikh, G.; Petrova, U.; Prikhodko, A.; Starodubtseva, N.; Chingin, K.; Chen, H.; Bugrova, A.; Kononikhin, A.; Bourmenskaya, O.; Brzhozovskiy, A.; et al. Vertical Transmission of SARS-CoV-2 in Second Trimester Associated with Severe Neonatal Pathology. *Viruses* **2021**, *13*, 447. [[CrossRef](#)]
81. Di Gennaro, F.; Murri, R.; Segala, F.V.; Cerruti, L.; Abdulle, A.; Saracino, A.; Bavaro, D.F.; Fantoni, M. Attitudes towards Anti-SARS-CoV2 Vaccination among Healthcare Workers: Results from a National Survey in Italy. *Viruses* **2021**, *13*, 371. [[CrossRef](#)]